Center–periphery organization of human object areas

Ifat Levy[1,2], Uri Hasson[2], Galia Avidan[1,3], Talma Hendler[4,5] and Rafael Malach[2]

[1] *The Interdisciplinary Center for Neural Computation, Hebrew University of Jerusalem, Jerusalem 91904, Israel*

[2] *Department of Neurobiology, Weizmann Institute of Science, Rehovot 76100, Israel*

[3] *Department of Neurobiology, Hebrew University of Jerusalem, Jerusalem 91904, Israel*

[4] *Functional Brain Imaging Laboratory, Wohl Institute for Advanced Imaging, Tel-Aviv Sourasky Medical Center, Tel Aviv 64239, Israel*

[5] *Faculty of Medicine, Tel Aviv University, Tel Aviv 69978, Israel*

Correspondence should be addressed to R.M. (bnmalach@wis.weizmann.ac.il)

The organizing principles that govern the layout of human object-related areas are largely unknown. Here we propose a new organizing principle in which object representations are arranged according to a central versus peripheral visual field bias. The proposal is based on the finding that building-related regions overlap periphery-biased visual field representations, whereas face-related regions are associated with center-biased representations. Furthermore, the eccentricity maps encompass essentially the entire extent of object-related occipito-temporal cortex, indicating that most object representations are organized with respect to retinal eccentricity. A control experiment ruled out the possibility that the results are due exclusively to unequal feature distribution in these images. We hypothesize that brain regions representing object categories that rely on detailed central scrutiny (such as faces) are more strongly associated with processing of central information, compared to representations of objects that may be recognized by more peripheral information (such as buildings or scenes).

During natural viewing, certain objects (such as faces) require detailed central scrutiny to perform such subtle visual tasks as detecting facial expressions and eye gaze directions. Larger objects (such as buildings or scenes) occupy a more peripheral field location, and can be recognized by their more peripheral-shape information. This distinction is further illustrated by the tendency of scanning eye movements to fixate face parts rather than background objects[1]. However, the potential role of this distinction in the organization of object representations has not been addressed so far.

Early visual areas of primates are retinotopically organized, so that the visual field is mapped in each area along two orthogonal axes: polar angle and eccentricity[2–6]. The center/periphery organization, that is, eccentricity mapping, is one of the most striking and robust organizational principles in the primate visual cortex. Both monkey and human cortices exhibit a meta-structure of center-periphery organization, in which similar distances from the fovea are mapped in stripes that are continuous across the entire ensemble of retinotopic visual areas[2–8]. The center/periphery organization extends into higher-order visual areas, whereas the polar angle representation in these areas is cruder, and orderly representations of the visual field meridians are absent[9,10]. Despite the evident importance of eccentricity maps, their possible relationship to object recognition has received little attention, and the possible effect of this organization on the way different object categories are represented in the human brain has not been studied.

Recently, the distinction between representation of faces and buildings has become a central issue in human visual cortex studies, due to the discovery that clearly distinct cortical regions are differentially activated by the two image categories: buildings acti-

vate a medial region along the collateral sulcus/parahippocampal gyrus[11–13], whereas faces activate a neighboring, more lateral region along the posterior fusiform gyrus[13–18]. The segregated representation of these object categories was attributed by some authors[11] to task- or semantics-related specialization, and by others[19] to their particular geometric information.

Here we report on an association between the two functional organizations found in human visual cortex: eccentricity maps and object categorization. Thus, we found that face-related regions are associated with central visual field representations, whereas building-related regions are associated with peripheral field representations. Furthermore, the center–periphery organization seems to encompass the entire constellation of high-order human object areas. Within the center–periphery maps, we found a hierarchical-like organization in that posterior regions manifested higher retinotopic bias compared to more anterior regions. Thus, our results unify two sets of findings in human visual cortex, eccentricity mapping and object selectivity, into a global principle of organization.

RESULTS

To explore the potential relationship between eccentricity maps and object selectivity, we first located face-related and building-related regions in the human visual cortex (experiment 1A). These regions were then superimposed onto the representation of visual field eccentricity in each subject (experiment 1B). To increase the sensitivity of high-order object areas to the visual field mapping, we constructed the retinotopic stimuli from a variety of natural object images (**Fig. 1**, see Methods[20]). We also mapped the horizontal and vertical visual field meridians that delineate borders of retinotopic areas[4,7,20,21] and superimposed the object areas on them.

Fig. 1. Stimuli used to map object-selective areas and eccentricity representations (experiments 1A and 2). Examples of stimuli used to map the face- and building-related areas and the center and periphery representations (see Methods for details). The center stimulus shown here was enlarged four times compared to the actual experiment, for presentation purposes.

Typically, face-related voxels were found in two foci (**Fig. 2a** and **b**): the lateral occipital region (LO) and the posterior fusiform gyrus (pFs). LO is situated ventrally and posteriorly to MT, extending into the posterior inferotemporal sulcus. Region pFs is anterior and lateral to areas V4/V8 (ref. 22), extending into the occipito-temporal sulcus, and corresponds to the fusiform face area (FFA) described previously[16]. Both foci largely overlapped the representation of the visual field center (**Fig. 2c**, yellow). Building-related voxels were found mainly in the collateral sulcus, where they partially overlapped an upper meridian representation and extended beyond it (**Fig. 2a** and **b**). This region largely overlapped the peripheral visual field representation (**Fig. 2c**, green) and sometimes extended to the mid visual field representation (**Fig. 2c**, purple), but always avoided the central field representation. Building-related voxels were also found in a dorsal region, in the vicinity of V3A and V7, where they often tended to overlap the periphery and mid representations.

In all the face-related regions, activation was significantly stronger in response to central stimuli compared to mid and peripheral stimuli (**Fig. 3**, LO, center versus periphery, $p < 0.005$, center versus mid, $p < 0.005$, $n = 12$, one-tailed paired t-test; pFs, center versus periphery, $p < 0.005$, center versus mid, $p < 0.05$, $n = 11$, one-tailed paired t-test). In analyzing the building-related regions, we included only voxels that both were selective to buildings compared to faces, and were anterior to areas V4/V8 (**Fig. 2b**). This region exhibited a high preference to the peripheral visual field representation compared to the central and mid ones (**Fig. 3**, Anterior CoS, periphery versus center, $p < 10^{-5}$, periphery versus mid, $p < 10^{-5}$, $n = 12$, one-tailed paired t-test).

To test the relationship between eccentricity and object categorization directly, we conducted another experiment, in which we mapped both center versus periphery and buildings versus faces during one scan (experiment 2). In the center and periphery conditions of this experiment, subjects viewed the exact same objects (see Methods), such that the two conditions only differed in the part of the visual field stimulated by the images and not in their shape features.

Again, face-related voxels were found in LO and in the pFs, where they overlapped the representation of the visual field center to a large extent, and building-related voxels were found mainly in the collateral sulcus, where they largely overlapped the peripheral visual field representation (**Fig. 4a**).

The Talairach[23] coordinates of the face- and building-related regions (**Table 1**) showed that our maps were in close correspondence to previous reports (buildings[11,13,24], faces[15,16,18,25]). The white circle in Fig. 2b shows the approximate position of face-related regions reported in early studies.

To make sure that subjects were able to recognize the objects in the peripheral stimuli, we conducted a behavioral experiment in which subjects were required to name the central and peripheral stimuli from experiment 2. The results showed that under the specific task of that experiment, there was a slight trend toward better recognition of objects in the center (mean ± s.d., $91 \pm 7\%$ correct responses) compared to the periphery ($86 \pm 9\%$ correct responses).

Thus, it is clear that a consistent association exists between the representation of particular object images and the central versus peripheral representation. However, it should be emphasized that the object representations were not homogenous: a clear indication of a hierarchical trend was observed, in that more posterior regions manifested a higher eccentricity bias compared to the most anterior regions. Thus, all face-related areas exhibited a significant central bias (**Fig. 4b**, LO, $p < 0.0005$; pFs, $p < 0.05$, $n = 5$, one-tailed paired t-test, center versus periphery). However, face-related foci located in LO showed a significantly higher central bias than those located in pFs. The ratio between activation to the

Fig. 2. Object-selective areas and visual field eccentricity maps. An example of face and building-related regions in one subject. (**a**) Preferential activation to faces versus buildings (red) and to buildings versus faces (blue) obtained in Experiment 1A, shown on sagittal, coronal and axial slices (left) and on a three-dimensional reconstructed brain (right). The color scales indicate the statistical correlation. The three-dimensional brain is shown in a ventral view. R, right; L, left; A, anterior; P, posterior. (**b**) The same regions from (**a**) are shown on the unfolded right hemisphere. Color scales are the same as in (**a**). White dotted lines denote borders of retinotopic visual areas V1, V2, V3, VP, V3A and V4/V8. The white circle surrounds the approximate locations of face-related activations reported in early studies[15,16,18,25]. LO, lateral occipital region; pFs, posterior fusiform gyrus; Ant. CoS, anterior collateral sulcus. (**c**) Borders of face-related (red) and building-related (blue) regions superimposed on central (yellow), mid (purple) and peripheral (green) visual field representations obtained in Experiment 1B. The face-related regions largely overlap the central visual field representation, whereas the building-related regions overlap the mid and peripheral ones but avoid the central visual field representation.
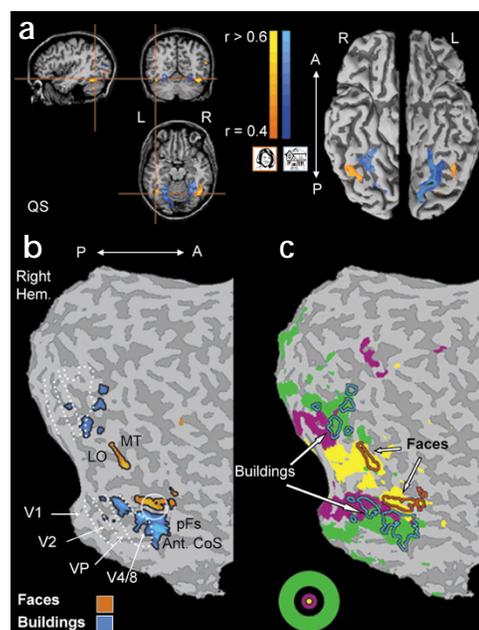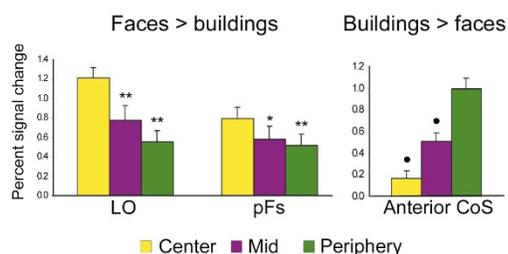
Fig. 3. Activation to different eccentricities in face- and building-related areas. Average signal from twelve subjects, experiment 1. Left, face-related voxels. Voxels were selected by applying a statistical test that searched for preferential activation for faces versus buildings (faces > buildings). Error bars, s.e.m. Asterisk ($p < 0.05$) and two asterisks ($p < 0.005$) denote significantly weaker activation compared to the center condition (one-tailed paired t-test; LO, $n = 12$; pFs, $n = 11$). Right, building-related voxels. Voxels were selected by applying the buildings > faces test. Only voxels that were outside the retinotopic areas were included. Error bars, s.e.m. Circle denotes significantly weaker activation compared to the periphery condition ($p < 10^{-5}$, $n = 12$, one-tailed paired t-test). Abbreviations as in Fig. 2.

center and periphery conditions was significantly higher in LO than in pFs ($p < 0.02$, one-tailed paired t-test). Activation ratio in the most anterior part of the face region in each subject (up to 3 voxels) was not significantly different from the ratio in the entire pFs ($p = 0.1$). The building-related area exhibited high preference to the peripheral visual field representation (**Fig. 4b**, $p < 0.002$, $n = 5$, one-tailed paired t-test). Comparing the center/periphery ratio between the entire area and its most anterior part (up to 3 voxels), showed no significant difference ($p = 0.1$).

The association of faces and buildings with central and peripheral representations may have emerged from the retinal center/periphery distribution of features in face and building images; for example, building images may tend to contain more low-level visual features such as edges and corners in the periphery than in the center. To test this possibility we conducted another experiment (experiment 3), in which subjects viewed pictures of buildings and faces as in experiment 2 (**Fig. 5**, 'regular'), but also pictures of larger faces and smaller buildings. These images were aimed at increasing the density of visual features in the periphery in the case of faces, and decreasing it in the case of buildings (Methods, **Fig. 5**). We compared the spectral energies of the central and peripheral parts of the images in each category (Methods, **Fig. 5**) and found that in the peripheral part of the visual field, the big-faces spectral energy was indeed higher than the energy of the small buildings.

As expected, in low-level retinotopic areas, which contain orderly representations of vertical and horizontal meridians (dotted lines in **Fig. 6a**), the activation pattern followed the retinal feature distribution in the images. Thus, 'large-face' selective voxels tended to overlap more peripheral field representations (green) compared to 'small-building' selective voxels, which activated more central representations (yellow). However, this trend was inverted in more anterior regions, outside the early retinotopic areas: the large-face selective voxels here overlapped central visu-

al field representations, whereas the small-buildings were associated with peripheral field representations.

Another way to analyze this experiment is to select voxels that were preferentially activated by regular faces compared to regular buildings and those that exhibited the opposite preference, and to examine their activation in response to large faces and small buildings (which were both ignored in the statistical tests). This analysis showed that face-related voxels were also activated by large faces (mean ± s.e.m., $1.4 \pm 0.1\%$) more than by small buildings ($0.6 \pm 0.1\%$; $p < 0.001$, $n = 6$, one-tailed paired t-test), whereas building-related voxels were activated by small buildings ($0.9 \pm 0.1\%$) more than by large faces ($0.4 \pm 0.1\%$; $p < 0.005$; **Fig. 6b**). Overall, these results clearly rule out the possibility that the center/periphery bias of faces and buildings is due to a difference in the retinal distribution of features in the images of these objects. However, voxels in the anterior collateral sulcus, which were preferentially activated by buildings compared to faces, also showed somewhat higher activation to large faces compared to regular ones. This preference can be expected from the peripheral visual field bias observed in this region.

To what extent can the center–periphery organization be extended to other object categories? To delineate the entire expanse of object-related cortex, we used a diverse set of objects and compared the activation produced by it with that produced by texture patterns (experiment 1). This contrast was shown previ-

Fig. 4. Simultaneous mapping of object areas and eccentricity representations. (**a**) Activation maps obtained from experiment 2 in the right hemispheres of two subjects. Borders of face- (red) and building- (blue) related areas are superimposed on central (yellow) and peripheral (green) representations. Dotted lines, borders of retinotopic visual areas. (**b**) Average signal from the five subjects who participated in experiment 2. Left, face-related voxels. Voxels were selected by applying a statistical test that searched for preferential activation for faces versus buildings (faces > buildings). Error bars, s.e.m. Asterisk ($p < 0.05$) and two asterisks ($p < 0.0005$) denote significantly stronger activation elicited by central stimuli compared to peripheral ones (one-tailed paired t-test). A significant central bias was demonstrated in all the face-related areas, although pFs showed less bias than LO. Right, building-related voxels. Voxels were selected by applying the buildings > faces test. Only voxels outside the retinotopic areas were included. Error bars, s.e.m. Circle denotes significantly stronger activation elicited by peripheral stimuli compared to central ones ($p < 0.002$, one-tailed paired t-test). Abbreviations as in Fig. 2.

articles
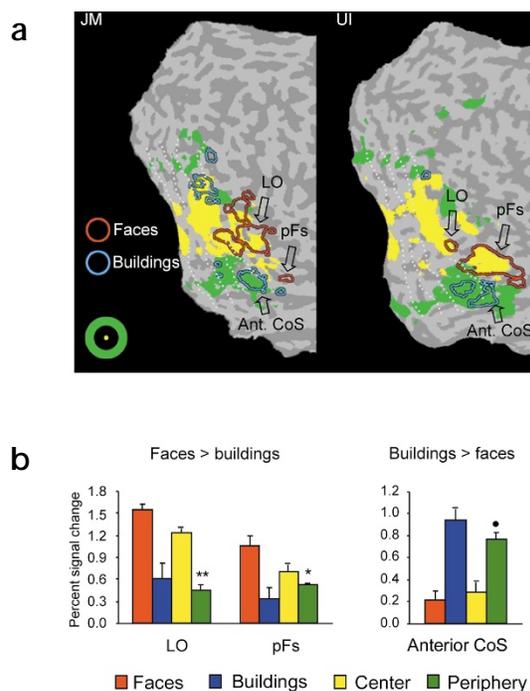
Table 1. Talairach[23] coordinates of face-related and building-related regions.

	Left hemisphere			Right hemisphere		
	x	*y*	*z*	*x*	*y*	*z*
Faces						
LO	−40 ± 10	−72 ± 3	−13 ± 10	41 ± 2	−69 ± 6	−10 ± 7
PFs	−38 ± 6	−50 ± 7	−21 ± 6	33 ± 6	−44 ± 8	−18 ± 4
Buildings						
Anterior CoS	−25 ± 1	−42 ± 3	−10 ± 2	25 ± 2	−39 ± 6	−12 ± 2

Values are mean ± s.d. in mm.

ously to be highly effective in delineating object-related cortex (the lateral occipital complex[26]). To maximize the statistical sensitivity of the test, we averaged the maps across 13 subjects (see Methods; **Fig. 7**). The entire constellation of occipito-temporal object areas stretching from the collateral sulcus medially to LO dorsally was highlighted, including face-related voxels, and a small region in the superior-temporal sulcus (**Fig. 7**). Due to the use of a bilateral surface coil, our mapping of more frontal and parietal regions was less certain in this figure.

To relate these areas to the eccentricity organization, we superimposed the borders of object-related cortex, averaged across 13 subjects, onto a center–periphery map obtained by averaging 12 of the same subjects (**Fig. 7b**). As can be seen, essentially the entire extent of occipito-temporal object areas was included in the center–periphery organization. More anteriorly, toward the anterior parahippocampal gyrus ventrally and the superior temporal sulcus dorsally, weakly activated patches appeared to lie outside the eccentricity map. This result indicates that although at present we cannot identify the exact pattern of activation that is related to each object category, we could conclude that most of its representation should be found somewhere within the bounds of the center–periphery global map.

DISCUSSION
Center–periphery organization in human object areas
Our results reveal an association between object images and the organization of visual field eccentricity. Thus, in high-order object areas, both large and small face images tended to be associated with central visual field representations (**Figs. 4a** and **6a**, red), whereas both large and small building images tended to overlap peripheral field representations (**Figs. 4a** and **6a**, blue). This association cannot be attributed to irregular mapping results, because both our maps of face and building-related regions, as well as our maps of central versus peripheral visual field representations, closely correlate with previously reported maps (faces[13–16,18,24,25,27], buildings[11,13,24], center/periphery[5,22]).

The finding of an eccentricity map in high-order object areas extends the previous report by our group of a foveal bias in the LOC[20]. The extension of the eccentricity maps to areas beyond the already characterized retinotopic areas[18,22] is most likely due to the use of object stimuli in the eccentricity mapping, rather than the texture-like stimuli typically used in earlier stud-

ies. Texture stimuli have been shown to be largely ineffective in activating high-order object areas[26].

The present result may seem to be at odds with previous work by our group, which showed substantial position and size invariance in the LOC[26,28]. However, this is not the case for the central-biased LOC, because changes in object image size or position, as long as they overlap the visual field center, are not expected to substantially affect the overall activation level (see also **Fig. 6**).

Macaque IT, which was suggested to be homologue to human LOC, has been shown to exhibit object selectivity[29,30] and to manifest a foveal bias[10,31–34]. A suggestion for a center/periphery segregation, compatible with the one described here, was found in posterior IT, in which the central visual field was represented more dorsally, and the peripheral visual field more ventrally[10,35]. However, these studies did not compare the feature/object selectivity in these regions, so it is unclear whether macaque IT actually exhibits an association between visual field and object selectivity similar to the one found here.

Although our results clearly point to a central versus peripheral bias in object-related, high-order areas, these regions did not exhibit a well-organized visual meridian representation[4,7,20] which is characteristic of early retinotopic areas. This result is again compatible with response properties of monkey IT neurons[10,35] as well as other neuroimaging results (for example, see ref 18).

A consequence of the physical distribution of features?
The central versus peripheral bias we observed could not be explained as a simple consequence of a center/periphery imbalance in the statistical distribution of visual features present in the face and building images used in our experiment. The relationship of faces and buildings to eccentricity maps was maintained even when the center/periphery balance of features was substantially modified by changing image size (**Fig. 5**; compare the spectral energy of the large faces and the small buildings). The peripheral bias did manifest itself in an enhancement of the activation for both buildings and faces when these were increased in size (**Fig. 6b**); however, this enhancement was not sufficient to overcome the shape-selective, preferential activation for buildings over faces characteristic of this region.
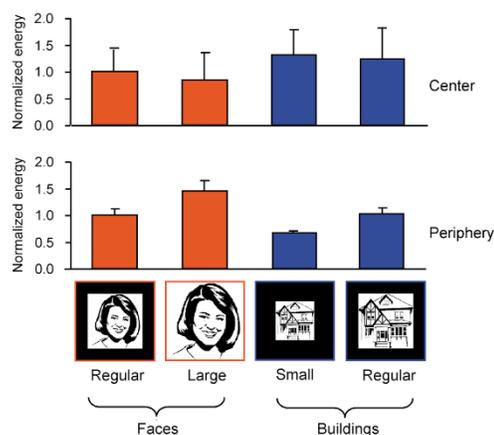
Fig. 5. Stimuli used in experiment 3. Average spectral energy of the central (top) and peripheral (bottom) parts of the images in each category of experiment 3. Energy was calculated as the sum of squares of amplitudes in the range 0.1–9 cycles/degree, in each image part. *y*-axis, normalized energy (see Methods). Error bars, s.d. In the peripheral part of the visual field, the energy in large face images was higher than the energy in small buildings.
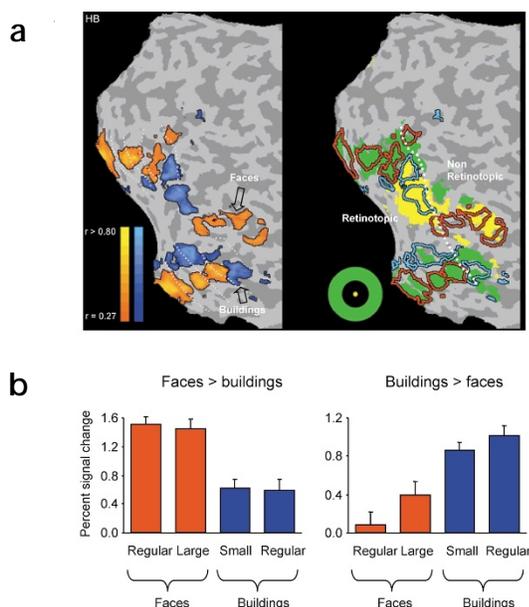
Fig. 6. Experiment 3, feature distribution experiment. (**a**) Results of experiment 3 in the right hemisphere of one subject. Red, voxels preferentially activated by large faces compared to small buildings; blue, voxels preferentially activated by small buildings compared to large faces. Left, object-selective areas superimposed on retinotopic borders, which are denoted by dotted lines. Color scales indicate the degree of statistical correlation. Right, the same areas superimposed on the eccentricity representation (yellow, center; green, periphery). Dotted line, estimated anterior border of retinotopic areas. Outside the retinotopic areas, the large-face voxels overlapped the central visual field representation, whereas the small buildings were associated with the peripheral field representation (indicated by arrows). (**b**) Average signal from the six subjects who participated in experiment 3. Left, voxels selected by applying a statistical test that searched for preferential activation for regular faces compared to regular buildings. Error bars, s.e.m. Right, voxels selected by applying the test 'regular buildings > regular faces.' Error bars, s.e.m. Large faces and small buildings were not included in the voxel selection test, and only voxels that were outside retinotopic areas were included in the analysis. The charts show that face-related voxels were also preferentially activated by large faces, and building-related voxels were also activated by small buildings.

Potential confounds

Additional factors that could have affected the results are attentional effects and eye movements. Attentional level was maintained across the various experimental conditions by using an identical task of equal attentional demand (1-back memory task) throughout the experiment (see experiment 1A, Methods). The clear retinotopy observed in our retinotopic and eccentricity maps rules out major eye movements during the scans. In addition, we obtained similar results using brief (250-ms) image presentations, which prevented extensive scanning eye movements (see experiment 2, Methods). Thus, our results cannot be attributed to differential eye movement in the different conditions.

In summary, our results unite two seemingly unrelated organizational features of human visual cortex, eccentricity maps and object selectivity, into a global organization in high-order occipito-temporal cortex.

Putative sources for the center-periphery organization

Such a center/periphery organization may have a developmental basis. During the layout of object representations, object categories are associated with the region of visual space that is attended during the establishment of these representations. Because faces require central scrutiny, possibly due to the minute differences in features that are critical for recog-

nition, they are associated with a central field bias, whereas buildings will be associated with a peripheral bias. In relation to this, expertise training in recognition of specific objects (for example, birds) leads to enhanced activation in face-related (and by implication, center-biased) cortical regions[25,36].

A complementary explanation is that the center/periphery organization allows for a more efficient allocation of processing resources for different object categories. Objects whose identification necessitates high acuity will receive more extensive inputs from the foveal representation, which provides the needed spatial resolution. In contrast, objects that can be recognized at a coarser level or that require large-scale integration of features will be associated with more peripheral representations. We would thus anticipate that representations of letters and digits (for example, refs. 14, 37), which strongly depend on foveal vision, will be associated with central field representations. We are currently exploring this prediction.

Fig. 7. Large-scale relationship of object-related cortex with center–periphery organization. (**a**) Preferential activation to objects versus patterns (red) and to patterns versus objects (blue) from 13 subjects (experiment 1). The results are presented on an inflated brain, shown in a ventral view (left) and on the unfolded hemispheres (right). Abbreviations as in Fig. 2; STS, superior temporal sulcus; PHG, parahippocampal gyrus. (**b**) Eccentricity maps from 12 subjects presented on an inflated brain shown in a ventral view (left) and on the unfolded hemispheres. Yellow, center; purple, mid; green, periphery. The borders of object areas from (**a**) were superimposed on the unfolded eccentricity map (red). Most of the object-related regions, with the exception of a few anterior foci, were contained within the center–periphery organization. Color scales indicate statistical correlation.

articles
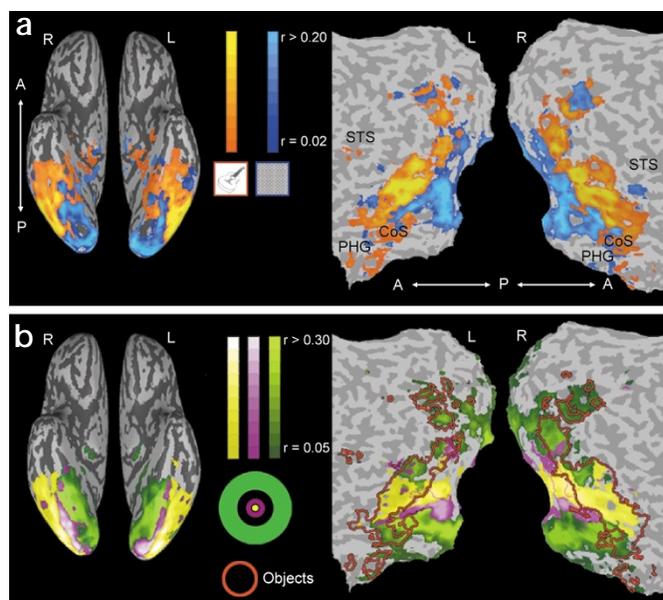
Relationship to other object categories?

Although we present data here regarding only two specific categories, buildings and faces, our results are also relevant to other object categories. This conclusion stems from the finding that substantial overlap occurred between the extent of object-selective occipito-temporal cortex and the center/periphery eccentricity maps. The implication of this large-scale correspondence is that any object category will have to be mapped somewhere along the eccentricity dimension and consequently will be associated, to some extent, with a particular combination of 'preferred' eccentricities.

The fact that different object classes are mapped according to a center/periphery rule does not exclude the possibility that additional stimulus dimensions may be mapped in an orderly manner within this cortical expanse[13]. Clearly, the face-related voxels do not overlap the entire center-biased regions, leaving room for other possible object categories. Similarly, various category-specific subdivisions may occur within the periphery-biased representation of the collateral sulcus (for example, Epstein and Kanwisher[19]).

Hierarchical organization within human object areas

The center–periphery organization described here provides a unified organizing principle for the entire extent of occipito-temporal, object-related cortex. However, this cortical expanse is not uniform. In particular, the more dorsal–posterior face-related regions seem to show a higher degree of central-field bias compared to the more ventral–anterior parts in the posterior fusiform gyrus (pFs), although the pFs did show a significant central bias (**Figs. 3** and **4b**), which was particularly evident when compared to the neighboring, peripherally biased collateral sulcus.

A similar hierarchical trend was also observed along the anterior–posterior axis of the collateral sulcus as one moves from V4/V8 toward the more anterior part of the sulcus. These results are compatible with our previous reports of a differential position and size selectivity within the LOC, whereby posterior regions showed a higher degree of sensitivity to these changes compared to anterior regions[28].

Following the acceptance of this work, a paper appeared[38] showing a center/periphery organization in dorsal LO using checker-board stimuli—thus providing additional confirmation to the prevalence of this organization in high-order visual areas.

METHODS

Subjects. Fourteen healthy subjects (8 women, 24–49 years old), participated in one or more of the experiments. All subjects had normal or corrected-to-normal vision and provided written informed consent. The Tel-Aviv Sourasky Medical Center approved the experimental protocol.

MRI acquisition. Subjects were scanned on a 1.5 Signa Horizon LX 8.25 GE scanner equipped with a quadrature surface coil (Nova Medical, Wakefield, Massachusetts), which covered the posterior brain regions. Blood oxygenation level dependent (BOLD) contrast was obtained with gradient-echo echo-planar imaging (EPI) sequence (TR, 3000, TE; 55; flip angle, 90°; field of view, 24×24 cm^2; matrix size $\times 80 \times 80$). The scanned volume included 17 nearly-axial slices of 4-mm thickness and 1-mm gap. T1-weighted high resolution ($1 \times 1 \times 1$ mm) anatomical images and a three-dimensional SPGR sequence were acquired for each subject to allow accurate cortical segmentation and reconstruction, and volume-based statistical analysis.

Visual stimuli. Stimuli were generated on a PC, projected onto a tangent screen positioned in front of the subject's forehead, and viewed through a tilted mirror.

Experiment 1. This experiment comprised two separate scans. In the first scan (experiment 1A), areas that showed preferential activation to common objects, faces or buildings were located ('objects scan'), and in the second scan (experiment 1B), eccentricity maps were obtained ('eccentricity scan'). Thirteen subjects participated in this experiment. The eccentricity scan of one subject was excluded due to problems in data acquisition.

In the objects scan (1A) subjects were presented with black and white drawings of faces, buildings, common objects and texture patterns shown in seven 9-s blocks of each category. The blocks were pseudo-randomly ordered and alternated with 6-s blanks. Each block consisted of 9 pictures, randomly ordered. The experiments included either 64 or 32 different pictures (4 and 9 subjects respectively). Each picture was presented for 800 ms followed by a blank interval of 200 ms. One or two pictures in each block were repeated, and subjects were asked to perform a 'one-back' matching task, while fixating on a central red point.

In the eccentricity scan (1B), subjects were presented with pictures of different objects, which were located in three eccentricities of the visual field: center (a circle of 1.4° diameter), mid (a ring of 2.5° inner diameter and 5° outer diameter) and periphery (a ring of 10° inner diameter and 20° outer diameter). Three types of central stimuli were used in separate epochs: faces, common objects (mainly animals) and written words. Pictures were presented in 18-s blocks, in which each picture was presented for 250 ms. Subjects were requested to fixate on a small fixation dot. Visual epochs alternated with 6-s blanks. Four cycles of the stimuli were shown.

Experiment 2. This experiment was designed to simultaneously map object-selective activation and center–periphery visual field bias (**Fig. 1**). Five subjects participated in the experiment. Line drawings of faces and buildings were used to locate object-selective areas (black and white, visual angle $12° \times 12°$). For the center–periphery mapping we used colored drawings of a variety of common objects. In the 'center' epochs, the stimuli were located in a circle at the center of the visual field (diameter, 1.8°). In the 'periphery' epochs, a number of copies (12–13) of the same object were placed within a ring confined to the peripheral visual field (11.5° inner diameter, 20° outer diameter, **Fig. 1**). Pictures of faces and buildings were presented in six blocks of 9 s each. Each block consisted of 18 different pictures. Thirty-six pictures of each type were used throughout the experiment. Each picture was presented for 250 ms followed by a blank interval of 250 ms. Central and peripheral pictures were presented in five 18-s blocks, in which each picture was presented for 250 ms. Seventy-two pictures of each type were used throughout the experiment. The visual stimulation blocks were ordered pseudo-randomly and alternated with 6-s blanks. A red fixation point was positioned centrally through the entire experiment, and subjects were instructed to fixate on it.

Experiment 3: Feature distribution experiment. Six subjects participated in this experiment. They were presented with pictures of faces and buildings as in experiment 2 ($12° \times 12°$) and with two additional categories: large faces (same faces, enlarged to a size of $17.5° \times 17.5°$) and small buildings (same buildings reduced to a size of $5.8° \times 5.8°$). Sixteen pictures of each category were used. Presentation procedure and task were the same as in experiment 1A.

Behavioral experiment. Six subjects participated in a behavioral experiment, which was conducted outside of the magnet six months after the fMRI scans. They were presented with the central and peripheral stimuli from experiment 2, and were asked to name them, while fixating on a red dot at the center of the screen. Each picture was presented for 250 ms followed by a 1250-ms blank. Percentages of correct responses were calculated.

Mapping borders of visual areas. The representations of vertical and horizontal visual field meridians were mapped in all subjects in order to delineate borders of retinotopic areas[4,7,20,21,39]. Visual stimulation was presented in 18-s blocks. Each image was presented for 250 ms. The stimuli consisted of triangular wedges that compensated for the expanded foveal representation. The wedges were presented either vertically (upper or lower vertical meridians) or horizontally (left or right horizontal meridians). The wedges consisted of either gray-level natural images or black and white objects-from-texture pictures[40]. Subjects were requested to fixate on a small central cross. Visual epochs alternated with 6-s blanks. Four cycles of the stimuli were shown.

Data analysis. fMRI data were analyzed with the BrainVoyager software package (R. Goebel, Brain Innovation, Masstricht, Netherlands) and with complementary in-house software. Each subject's data from each scan were analyzed separately (except for the multi-subject analysis, see below). The functional images were superimposed on two-dimensional anatomical images and incorporated into the three-dimensional data sets through trilinear interpolation. The complete data set was transformed into Talairach[23] space. Preprocessing of functional scans included three-dimensional motion correction and high-frequency temporal filtering. Statistical analysis was based on the General Linear Model[41].

The cortical surface was reconstructed from the three-dimensional SPGR scan, unfolded, cut along the calcarine sulcus, and flattened. The obtained activation maps were superimposed on the unfolded cortex and the Talairach coordinates were determined for the center of each ROI.

The two-dimensional Fourier transforms (FT) of the images in experiment 3 were calculated using the Matlab 5.3 software (Mathworks, Natick, Massachusetts, 1999) according to the following formula:

$$X\,(u,\,v) = \sum_{j=0}^{N-1}\sum_{k=0}^{N-1} x(j,\,k)\,e^{-\frac{2\pi i}{N}(ju+kv)}$$

Here, X is the FT, x is the image and $N \times N$ is the image size.

FT was computed separately for the central part of each image and the peripheral part. The square amplitudes of frequencies between 0.1 and 9 cycles/degree in each image part were summed (total energy):

$$E = \sum \left| A(i,\,j) \right|^2$$

Here, E is the total energy and the summation is over the frequencies in the above range.

The bar charts in Fig. 5 present the mean total energy in the central and peripheral parts of each category, normalized by the regular faces total energy.

Multi-subject analysis. The object-areas map in Fig. 7 was obtained from 13 subjects. The eccentricity map was obtained from 12 of these subjects. To create the maps, the time courses of all subjects were transformed into Talairach space, z-normalized and concatenated, and the statistical tests were done on the concatenated time course.

1. Yarbus, A. L. *Eye Movements and Vision* (Plenum, New York, 1967).
2. Gattass, R., Gross, C. G. & Sandell, J. H. Visual topography of V2 in the macaque. *J. Comp. Neurol.* **201**, 519–539 (1981).
3. Gattass, R., Sousa, A. P. & Gross, C. G. Visuotopic organization and extent of V3 and V4 of the macaque. *J. Neurosci.* **8**, 1831–1845 (1988).
4. DeYoe, E. A. *et al.* Mapping striate and extrastriate visual areas in human cerebral cortex. *Proc. Natl. Acad. Sci. USA* **93**, 2382–2386 (1996).
5. Tootell, R. B. H. *et al.* Functional analysis of V3A and related areas in human visual cortex. *J. Neurosci.* **71**, 7060–7078 (1997).
6. Engel, S. A., Glover, G. H. & Wandell, B. A. Retinotopic organization in human visual cortex and the spatial precision of functional MRI. *Cereb. Cortex* **7**, 181–192 (1997).
7. Sereno, M. I. *et al.* Borders of multiple visual areas in humans revealed by functional magnetic resonance imaging. *Science* **268**, 889–893 (1995).
8. Rosa, M. G. in *Extrastriate Cortex in Primates* (eds. Rockland, K. S., Kaas, J. & Peters, A.) 127–203 (Plenum, New York, 1997).
9. Desimone, R. & Ungerleider, L. G. Multiple visual areas in the caudal superior temporal sulcus of the macaque. *J. Comp. Neurol.* **248**, 164–189 (1986).
10. Boussaoud, D., Desimone, R. & Ungerleider, L. G. Visual topography of area TEO in the macaque. *J. Comp. Neurol.* **306**, 554–575 (1991).
11. Aguirre, G. K., Zarahn, E. & D'Esposito, M. An area within human ventral cortex sensitive to "building" stimuli: evidence and implications. *Neuron* **21**, 373–383 (1998).
12. Epstein, R. & Kanwisher, N. A cortical representation of the local visual environment. *Nature* **392**, 598–601 (1998).
13. Ishai, A., Ungerleider, L. G., Martin, A., Schouten, H. L. & Haxby, J. V. Distributed representation of objects in the human ventral visual pathway. *Proc. Natl. Acad. Sci. USA* **96**, 9379–9384 (1999).
14. Puce, A., Allison, T., Asgaei, M., Gore, J. C. & McCarthy, G. Differential sensitivity of human visual cortex to faces, letterstrings and textures: a functional magnetic resonance imaging study. *J. Neurosci.* **16**, 5205–5215 (1996).
15. Clark, V. P. *et al.* Functional magnetic resonance imaging of human visual cortex during face matching: a comparison with positron emission tomography. *Neuroimage* **4**, 1–15 (1996).
16. Kanwisher, N., McDermott, J. & Chun, M. M. The fusiform face area: a module in human extrastriate cortex specialized for face perception. *J. Neurosci.* **17**, 4302–4311 (1997).
17. McCarthy, G., Puce, A., Gore, J. C. & Allison, T. Face specific processing in the human fusiform gyrus. *J. Cogn. Neurosci.* **9**, 605–610 (1997).
18. Halgren, E. *et al.* Location of human face-selective cortex with respect to retinotopic areas. *Hum. Brain Mapp.* **7**, 29–37 (1999).
19. Epstein, R., Harris, A., Stanley, D. & Kanwisher, N. The parahippocampal place area: recognition, navigation, or encoding? *Neuron* **23**, 115–125 (1999).
20. Grill-Spector, K. *et al.* A sequence of object-processing stages revealed by fMRI in the human occipital lobe. *Hum. Brain Mapp.* **6**, 316–328 (1998).
21. Engel, S. A. *et al.* fMRI of human visual cortex. *Nature* **369**, 525 (1994).
22. Hadjikhani, N., Liu, A. K., Dale, A. M., Cavanagh, P. & Tootell, R. B. Retinotopy and color sensitivity in human visual cortical area V8. *Nat. Neurosci.* **1**, 235–241 (1998).
23. Talairach, J. & Tournoux, P. *Co-Planar Stereotaxic Atlas of the Human Brain* (Thieme Medical, New York, 1988).
24. Haxby, J. V. *et al.* The effect of face inversion on activity in human neural systems for face and object perception. *Neuron* **22**, 189–199 (1999).
25. Gauthier, I., Tarr, M. J., Anderson, A. W., Skudlarski, P. & Gore, J. C. Activation of the middle fusiform 'face area' increases with expertise in recognizing novel objects. *Nat. Neurosci.* **2**, 568–573 (1999).
26. Malach, R. *et al.* Object-related activity revealed by functional magnetic resonance imaging in human occipital cortex. *Proc. Natl. Acad. Sci. USA* **92**, 8135–8139 (1995).
27. Hoffman, E. A. & Haxby, J. V. Distinct representations of eye gaze and identity in the distributed human neural system for face perception. *Nat. Neurosci.* **3**, 80–84 (2000).
28. Grill-Spector, K. *et al.* Differential processing of objects under various viewing conditions in the human lateral occipital complex. *Neuron* **24**, 187–203 (1999).
29. Tanaka, K. Neuronal mechanisms of object recognition. *Science* **262**, 685–688 (1993).
30. Tanaka, K. Inferotemporal cortex and object vision. *Annu. Rev. Neurosci.* **19**, 109–139 (1996).
31. Gross, C. G., Bender, D. B. & Rocha-Miranda, C. E. Visual receptive fields of neurons in inferotemporal cortex of the monkey. *Science* **166**, 1303–1306 (1969).
32. Seltzer, B. & Pandya, D. N. Afferent cortical connections and architectonics of the superior temporal sulcus and surrounding cortex in the rhesus monkey. *Brain Res.* **149**, 1–24 (1978).
33. Desimone, R., Fleming, J. & Gross, C. G. Prestriate afferents to inferior temporal cortex: an HRP study. *Brain Res.* **184**, 41–55 (1980).
34. Baizer, J. S., Ungerleider, L. G. & Desimone, R. Organization of visual inputs to the inferior temporal and posterior parietal cortex in macaques. *J. Neurosci.* **11**, 168–190 (1991).
35. Hikosaka, K. Representation of foveal visual fields in the ventral bank of the superior temporal sulcus in the posterior inferotemporal cortex of the macaque monkey. *Behav. Brain Res.* **96**, 101–113 (1998).
36. Gauthier, I., Skudlarski, P., Gore, J. C. & Anderson, A. W. Expertise for cars and birds recruits brain areas involved in face recognition. *Nat. Neurosci.* **3**, 191–197 (2000).
37. Gauthier, I. *et al.* The fusiform "face area" is part of a network that processes faces at the individual level. *J. Cogn. Neurosci.* **12**, 495–504 (2000).
38. Tootell, R.B. & Hadjikani, N. Where is 'dorsal v4' in human visual cortex? retinopic, topographic and functional evidence. *Cereb. Cortex* **11**, 298–311 (2001).
39. Grill-Spector, K., Kushnir, T., Hendler, T. & Malach, R. The dynamics of object-selective activation correlate with recognition performance in humans. *Nat. Neurosci.* **3**, 837–843 (2000).
40. Grill-Spector, K., Kushnir, T., Edelman, S., Itzchak, Y. & Malach, R. Cue-invariant activation in object-related areas of the human occipital lobe. *Neuron* **21**, 191–202 (1998).
41. Friston, J. *et al.* Statistical parametric maps in functional imaging: a general linear approach. *Hum. Brain Mapp.* **2**, 189–210 (1995).